SCIENCE CHINA
Information Sciences

December 2019, Vol. 62 220404:1–220404:8
https://doi.org/10.1007/s11432-019-1474-3

• RESEARCH PAPER •
Special Focus on Two-Dimensional Materials and Device Applications

Nonvolatile memristor based on heterostructure of 2D room-temperature ferroelectric α-In_2Se_3 and WSe_2

Huai YANG[1,2], Mengqi XIAO[1,2], Yu CUI[1,2], Longfei PAN[1,2], Kai ZHAO[1,2] & Zhongming WEI[1,2*]

[1]*State Key Laboratory of Superlattices and Microstructures, Institute of Semiconductors, Chinese Academy of Sciences, Beijing* 100083*, China;*
[2]*Center of Materials Science and Optoelectronics Engineering, University of Chinese Academy of Sciences, Beijing* 100083*, China*

Received 2 June 2019/Revised 18 July 2019/Accepted 24 July 2019/Published online 30 October 2019

Abstract Two-dimensional (2D) ferroelectricity is considered to have significant potential for information storage in the future. Semiconducting ferroelectrics that are stable at room temperature afford many possibilities for the assembly of various high-performance heterostructures and fabricating multifuntional devices. Herein, we report the synthesis of a stable van der Waals (vdW) single-crystal semiconductor α-In_2Se_3. Piezoresponse force microscopy (PFM) measurements demonstrated the out-of-plane ferroelectricity in ∼15 layers α-In_2Se_3 at room temperature. Both ferroelectric domains with opposite polarization and the tested amplitude and phase curve proved that this semiconductor exhibits hysteresis behavior during polarization. In the α-In_2Se_3/WSe_2 vertical heterostructure device, the switchable diode effect and nonvolatile memory phenomenon showed a high on/off ratio and a small switching voltage. The distinct resistance switches were further analyzed by band alignment of the heterostructure under different polarizations by first principle calculations. Nonvolatile memory based on vdW ferroelectric heterostructure could provide a novel platform for developing 2D room-temperature ferroelectrics in information storage.

Keywords 2D ferroelectricity, α-In_2Se_3, heterostructure, nonvolatile memristor, polarization

Citation Yang H, Xiao M Q, Cui Y, et al. Nonvolatile memristor based on heterostructure of 2D room-temperature ferroelectric α-In_2Se_3 and WSe_2. Sci China Inf Sci, 2019, 62(12): 220404, https://doi.org/10.1007/s11432-019-1474-3

1 Introduction

Ferroelectric memories based on nonvolatile resistance switching (NVRS) have significant potential to be applied in the modern electronic information industries [1–3]. By applying voltage to polarize the ferroelectric, its resistance can be modulated between a high-resistance state and a low-resistance state, which are subsequently retained and represent "1" and "0" without any further power supply for information storage [4]. Transitional ferroelectric films such as lead zirconate titanate (PZT) and $BaTiO_3$, which have wide bandgaps, are restricted in memory devices since they usually serve as dielectric layers applied to the capacitor during charging and discharging [5, 6]. Recently developed two-dimensional van der Waals (vdW) materials and their heterostructures provide a novel platform for next-generation multifunctional devices due to their optical [7], electronic [8], thermal [9], and magnetic properties [10]. For example, 2D

* Corresponding author (email: zmwei@semi.ac.cn)

ferroelectricity in vdW crystals may be applied to nonvolatile ferroelectric memories, negative capacitors, and artificial synapses and sensors [2, 11–14].

Since the discovery of 2D ferroelectric SnTe, 2D ferroelectrics have drawn attention on account of the possibilities for their integration and their performance [15]. However, 2D SnTe exhibits a relatively low ferroelectric transition temperature (T_c) below room temperature, limiting its application to ferroelectric devices [15]. It has been reported that 2D vdW insulator $CuInP_2S_6$ may undergo out-of-plane polarization at room temperature, and this may be applied to ferroelectric field-effect transistors (Fe-FETs) based on the $MoS_2/CuInP_2S_6$ heterostructure [16, 17]. Recently, stable, high-performance ferroelectric In_2Se_3 has been reported to undergo room-temperature out-of-plane and in-plane ferroelectricity down to the monolayer scale [18]. Semiconducting In_2Se_3 has been used for phase-change storage, thermoelectric, and photoelectric applications [19–21]. Nonetheless, the application of two-dimensional ferroelectric α-In_2Se_3 on heterostructure for nonvolatile memory remains a largely unexplored challenge.

In this paper, high-quality In_2Se_3 crystals have been synthesized by chemical vapor transport (CVT) methods. The obtained In_2Se_3 belongs to the ferroelectric α-phase with rhombohedral R3 m space groups and exhibits perfect single crystallinity according to Raman spectroscopy and high-resolution transmission electron microscope (HRTEM) analyses. Piezoresponse force microscopy (PFM) test demonstrated room-temperature stable out-of-plane ferroelectricity in α-In_2Se_3 composed of ∼15 layers. The scanned ferroelectric domains displayed opposite polarization orientation and the tested amplitude and phase curve exhibited obvious hysteresis in the reversal process. Assembled In_2Se_3/WSe_2 heterostructure showed obvious switchable rectifying effects and nonvolatile memory phenomena. Rectifying I-V behavior can be reversed by applying an opposite voltage between the heterostructure and the I-V curve then showed hysteresis and resistance switches at −4.5 V. Two-dimensional nonvolatile memory based on α-In_2Se_3/WSe_2 vdW heterostructure may provide a new opportunity and platform for utilizing and developing 2D ferroelectric materials in large-scale modern information storage.

2 Experimental

Ferroelectric α-In_2Se_3 crystals were synthesized using CVT methods with iodine as the transport agent. High-purity In powder (aladdin, 99.99%), Se powder (aladdin, 99.99%) and I pellets (aladdin, 99.99%) were weighed in stoichiometric ratios and mixed in an ampoule. The ampoule was sealed under low-pressure conditions in a pumping and sealing system (ZKKY F-100/150). Thereafter, the growth temperature was set to 700°C (lower zone) or 800°C (higher zone) using a horizontal double-zone tube furnace system, in order to promote chemical combination for 3 days, at then at 800°C (lower zone) and 950°C (higher zone) to grow the crystals for 10 days [22]. The system was finally cooled down to room temperature at a rate of 10°C/h. The resulting crystals had lengths of 0.2 to 1 cm. The α-In_2Se_3 flakes derived from the ampoule were attached onto Scotch tape and we exfoliated the α-In_2Se_3 crystals to a few layers on a SiO_2/Si substrate for Raman spectroscopy measurements, in order to obtain the desired ratio and phase of the crystal. The fewlayer In_2Se_3 nanoflakes were transferred onto Cu foil using PMMA-assist methods and HRTEM was used to investigate their structure and lattice arrangement. After this, we exfoliated 5–70 nm In_2Se_3 onto a Pt/Si substrate to determine its ferroelectric properties using PFM measurement using a Bruker dimension ICON instrument. Finally, by assembling the α-In_2Se_3/WSe_2 heterojunction, we fabricated a nonvolatile memory based on the ferroelectricity of α-In_2Se_3 and measured the properties of the memory using an Agent B1500 system.

3 Results and discussion

In_2Se_3 is a two-dimensional van der Waals material, and is a typical semiconductor with a direct band gap of approximately 1.3 eV [23]. The successful synthesis of ferroelectric α-phase In_2Se_3 is a significant challenge in that there are at least five known crystal forms (α, β, γ, δ and κ phases) [19]. Figure 1(a) shows the structure of typical ferroelectric α-phase In_2Se_3. For an individual In_2Se_3 layer, five triangular

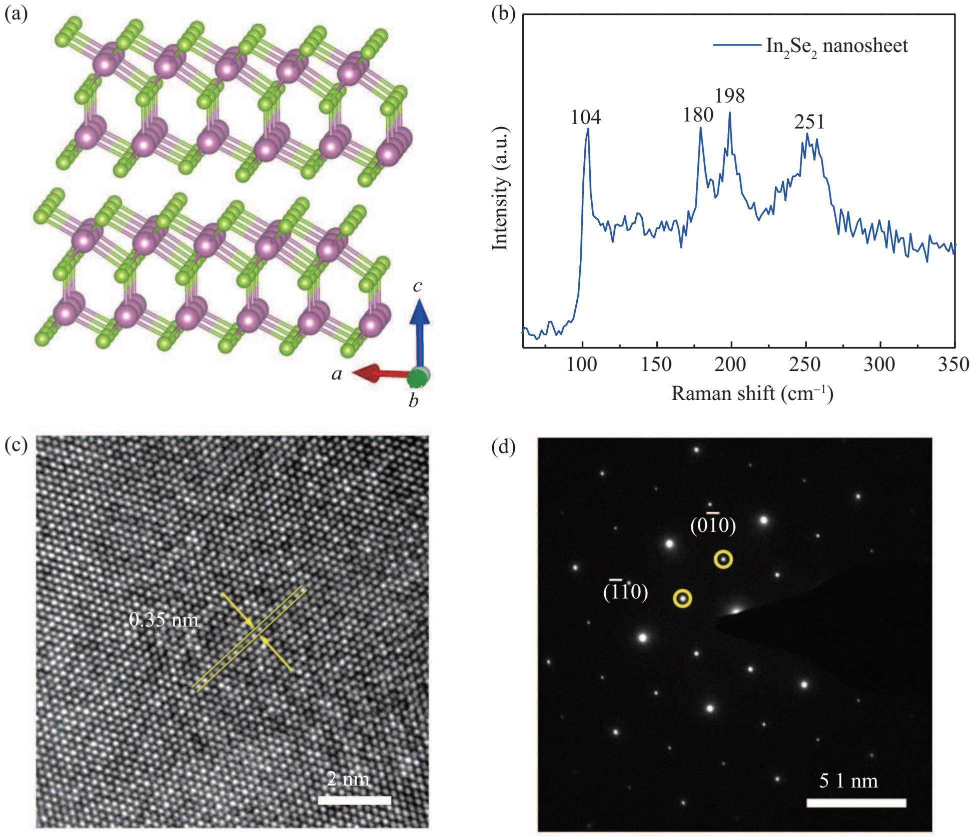

Figure 1 (Color online) Basic structure and characterization of ferroelectric α-In_2Se_3. (a) Atomic structure of layered α-In_2Se_3 crystals; (b) Raman spectra of ∼10 nm α-In_2Se_3 nanosheet; (c) high-resolution TEM image of exfoliated In_2Se_3; (d) SAED patterns of the α-In_2Se_3 nanoflake corresponding to (c).

atomic lattices in the sequence Se-In-Se-In-Se lattices are connected by covalent bonds. In the case of the bulk crystal, this belongs to the R3 m space group, and the In_2Se_3 layers are stacked by van der Waals force [24]. R3 m and P63/mmc space groups of α-In_2Se_3 samples have been previously reported in [24,25] and both exhibit ferroelectricity. As shown in Figure 1(a), the middle Se atom in the asymmetric position breaks the centrosymmetry of the structure, thus fulfilling the prerequisite of inversion symmetrybreaking in ferroelectrics [26]. The dramatic difference in the interlayer spacing between the middle Se layer and the two In layers contributes to the net electric dipole in the out-of-plane direction. Thus, the out-of-plane ferroelectric polarization orientation in α-In_2Se_3 has two degenerated states: the upward and downward directions. After applying an external electric field between the α-In_2Se_3 layer, the atomic position of middle-layer Se atoms deviated from the inversion center of the quintuple layers, and the orientation of ferroelectric polarization switches [26].

In order to affirm the exact phase and structure of the synthesized In_2Se_3 crystals, they were exfoliated onto SiO_2/Si substrates using Scotch tape. The color of exfoliated In_2Se_3 crystals was estimated based on previous experience. The thick layers on the substrate is shown golden yellow while thin layer is light blue. We obtained few-layer In_2Se_3 nanoflakes that were identifiable by optical microscopy and analyzed by Raman spectroscopy using a 532 nm laser. The Raman spectra of as-grown In_2Se_3 flakes is shown in Figure 1(b), where three main peaks at 104, 180 and 200 cm^{-1} are observed in the sample. Based on [27], the peak in 104 cm^{-1} can be attributed to the A_1 symmetry vibration in α-In_2Se_3. The peaks at 180 and 200 cm^{-1} are attributed to the A_1(TO), and A_1(LO + TO) phonon modes of In_2Se_3, respectively. This demonstrates that the obtained In_2Se_3 crystals belong to α-In_2Se_3 instead of the reported β-In_2Se_3, the latter of which lacks ferroelectric properties [20]. To completely investigate the structure and crystallinity of our synthesized In_2Se_3, high-resolution TEM was employed to examine the ferroelectric nanoflake. HRTEM lattice fringes and spot patterns in selected area electron diffraction

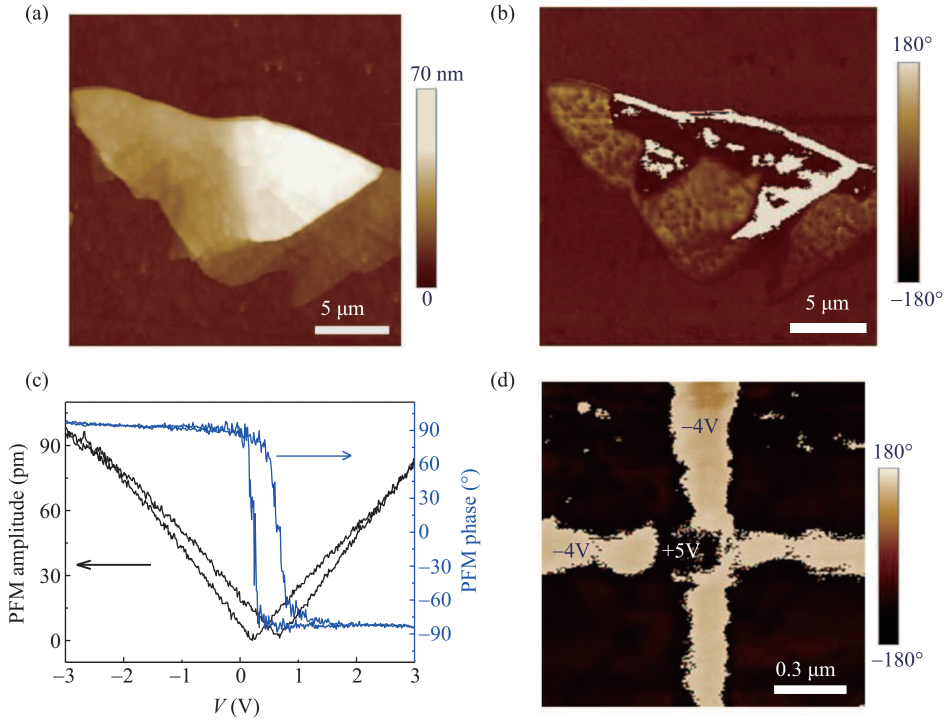

Figure 2 (Color online) PFM investigation of as-grown α-In_2Se_3 on a Pt/Si substrate. (a) AFM image of typical thin flakes with thicknesses between 5 and 70 nm. (b) Corresponding PFM phase image. Polarization reversal under external electrical field. (c) On-field PFM amplitude and PFM phase hysteresis loops on a 20 nm thick flake. (d) Corresponding PFM phase image of a ~15 layer In_2Se_3 nanosheet, two rectangular strip domains are first written with −4 V on the sample, then the middle square domain is written with +5V. The clear phase change proves that the ferroelectric domain can be flipped by the applied voltage.

(SAED) demonstrated the single-crystal nature of the flakes shown in Figure 1(c) and (d). Furthermore, SAED results indicated that the crystal belongs to the rhombohedral structure and has R3 m (No. 160) symmetry. The HRTEM image shows anticipative rhombohedral lattice fringes with a lattice spacing of approximately 0.35 nm, consistent with the lattice spacing of (110) planes in the simple R3 m phase according to theoretical crystal structure [24].

To investigate the spontaneous polarization originating from the broken inversion symmetry and polar structure of α-In_2Se_3, we carried out PFM measurement by exfoliating α-In_2Se_3 crystals on conductive Pt/Si substrates. Atomic force microscope (AFM) images and corresponding out-of-plane PFM phase images are shown in Figure 2(a) and (b), respectively. The phase image reveals two out-of-plane polarization directions with opposite phase contrasts in the α-In_2Se_3 flake, which is independent of the sample thickness inferred from the AFM contrast. The deep and shallow regions exhibit α-phase difference of 180°, corresponding to ferroelectric domains with upward and downward polarization vectors perpendicular to the horizontal plane, respectively. In order to further investigate the ferroelectric hysteresis behavior of α-In_2Se_3 nanosheets, we applied an electric field across the top of the material using a conducive Pt/Ir tip. The butterfly-like loops and hysteresis loops are presented in Figure 2(c). This indicated that an imposed direct current (DC) voltage in the tip ranging from −3 V to 3 V was sufficient to reverse the polarization of domains. The butterfly-like voltage-dependent amplitude loop exhibited an opening voltage of ~0.8 V and amplitude change of approximately 90 pm, corresponding to 180° phase switching. The asymmetry of the amplitude loop contributes to the leakage of a high concentration of free carrier.

The inversion and hysteresis of the both curves indicates that the orientation of ferroelectric polarization can be controlled artificially using the applied electric field. Figure 2(d) shows the PFM phase images of ferroelectric domains written onto the few-layer α-In_2Se_3. The two long rectangle strips were written by scanning the grounded AFM tip with a negative voltage −4 V applied to the bottom electrode.

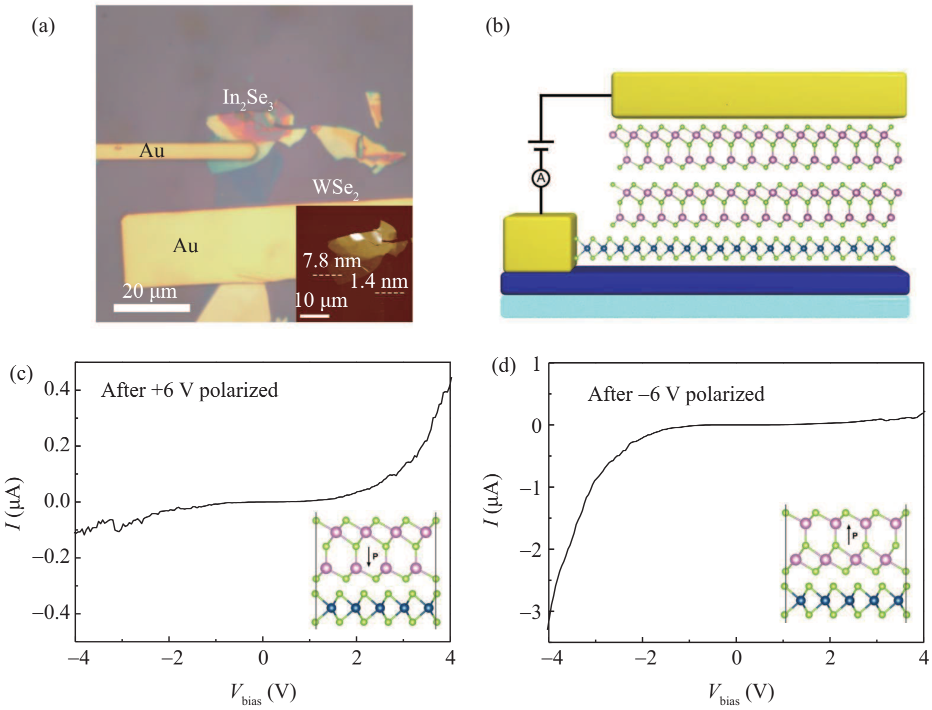

Figure 3 (Color online) (a) Optical and AFM images of the α-In_2Se_3/WSe_2 vertical heterostructure device; (b) schematic diagram of the corresponding device; (c), (d) *I*-*V* curves for a ferroelectric memorizer with switchable rectifying behavior.

An opposite phase shift was observed, indicating upward polarization of the domains. Furthermore, by applying a positive voltage of +5 V, the middle square domain with upward polarization can be switched back to its original state. The image after writing shows an enduring rectangle and square pattern, demonstrating the nonvolatile memory property of ferroelectric polarization in α-In_2Se_3 nanoflakes.

The ferroelectric α-In_2Se_3 nanoflakes were further employed in nonvolatile memory by assembling an α-In_2Se_3/WSe_2 heterojunction. The few-layer α-In_2Se_3 flakes were mechanically exfoliated from as-grown bulk crystals and transferred to SiO_2 (300 nm)/Si substrates. These WSe_2 flakes were mechanically exfoliated using Scotch tape and transferred onto a piece of Polydimethylsiloxane (PDMS). The heterostructure was assembled using a transfer station, where WSe_2 on PDMS was installed on a glass slide and aligned on the α-In_2Se_3 flake. The fabricated heterojunction was measured by AFM to determine its thickness. Figure 3(a) and (b) shows a schematic diagram of a typical heterostructure and an optical microscope image of the nonvolatile memory device. An AFM image of the α-In_2Se_3/WSe_2 heterojunction is shown in the inset of Figure 3(b), indicating that α-In_2Se_3 and WSe_2 nanoflakes have thicknesses of 7.8 and 14 nm, corresponding to several layer and bilayer flakes, respectively. The Au electrodes were then transferred on the α-In_2Se_3 and WSe_2 to avoid damage to the crystal structure, as determined in previous research. The memory device was tested by applying the electric field across the Au electrodes.

Figure 3(c) and (d) shows typical *I*-*V* curves of the storage characteristic of α-In_2Se_3/WSe_2 heterojunctions after DC bias at ±6 V voltage was applied to change the polarization orientation of ferroelectric α-In_2Se_3, revealing a nonvolatile resistance switching in the heterojunction. After applying a DC bias at +6 V, the device showed forward rectifying behavior, whereas applying a DC bias at −6 V bias resulted in the reversal of this behavior and showed instead a backward rectifying effect. The flow of current through the top electrode to the lower electrode was significantly improved after applying a DC bias at −6 V to polarize the ferroelectric α-In_2Se_3 layers. This phenomenon can be explained in terms of the polarization direction of the ferroelectric α-In_2Se_3 layers and the band alignment of the vertical heterostructure. Applying a DC bias from two electrodes will produce a reversible built-in electric field in nanoflakes of α-In_2Se_3, which have the ability to switch their polarized direction between the "up" and "down" orientations.

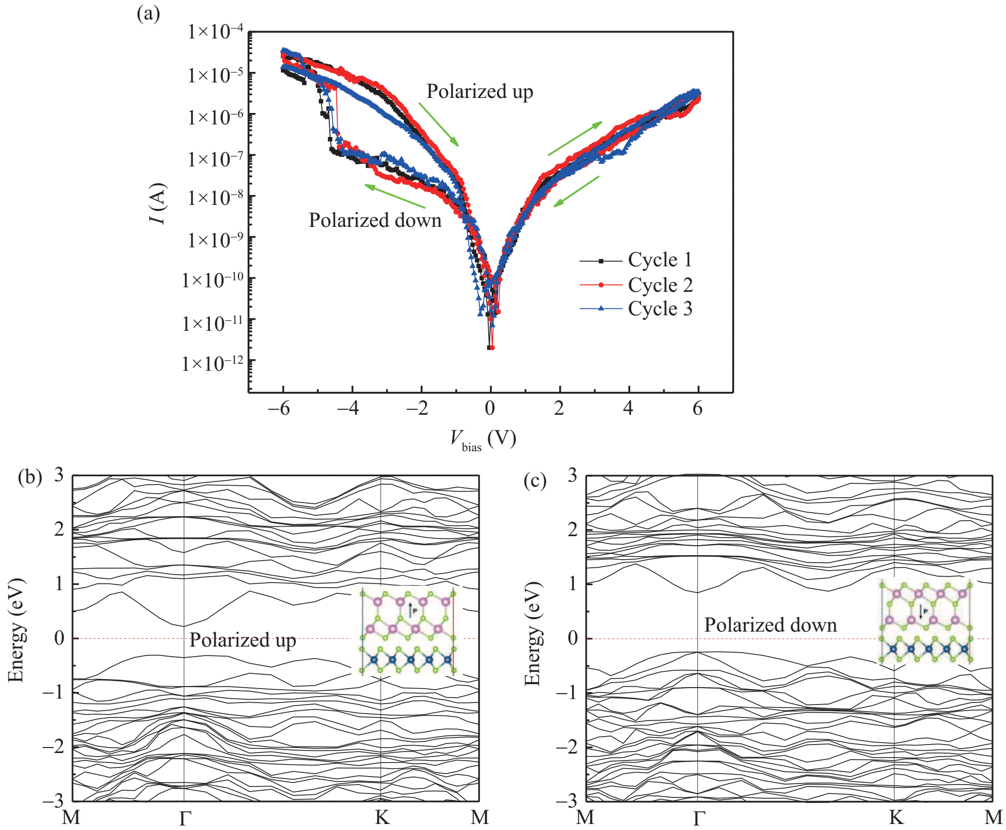

Figure 4 (Color online) (a) *I*-*V* curves measured under high DC bias, showing hysteresis characteristics. The calculated band alignment of the α-In_2Se_3/WSe_2 heterostructure after being polarized up (b) and polarized down (c), respectively.

The *I*-*V* characteristics of the α-In_2Se_3/WSe_2 heterostructure under high DC bias were further studied by circulatory *I*-*V* measurement. *I*-*V* curves were obtained by sweeping the bias voltage from −6 V to +6 V and then back to −6 V. To ensure complete switching of the ferroelectric polarization direction, the sweeping rate was maintained at a relatively low level about 1.5 V per second. As shown in Figure 4(a), *I*-*V* curves under negative voltage show distinct hysteresis behavior, indicating a resistive switching effect. While under positive voltage, the *I*-*V* curves show inconspicuous hysteresis. Asymmetric hysteresis behavior can be attributed to the Schottky barrier between the Au electrode and WSe_2 layer when current flows from the top to bottom layers. The difference of on/off state indicates that the resistance of the heterostructure with polarization 'down' was 100 times that of the resistance with polarization 'up' under negative voltage. It can therefore be speculated that the band alignment of α-In_2Se_3/WSe_2 heterostructure was dramatically changed, resulting in a nonvolatile resistance switching phenomenon.

To verify this, we employed first principle band alignment calculation of simulative α-In_2Se_3/WSe_2 heterostructures under different polarization using Vienna Ab-initio simulation package (VASP) [18]. The large reduction of conductance can be explained by variations in bandgap for the vertical heterostructure. We also calculated the band alignment of the simplified α-In_2Se_3/WSe_2 bilayer to verify the variation in bandgap between different polarization directions in the ferroelectric layer. As shown in Figure 4(b) and (c), when the applied high positive DC bias between the heterostructure exceeded 4.5 V, the polarization direction of ferroelectric α-In_2Se_3 was switched to 'up', indicating an 'on' state and corresponding to the calculated bandgap value of approximately 0.53 eV for the α-In_2Se_3/WSe_2 bilayer. However, when a higher negative DC bias was applied between the heterostructure, the polarization direction of ferroelectric α-In_2Se_3 was reversed to 'down', indicating an 'off' state corresponding to a larger calculated bandgap value of approximately 1.09 eV. The large increase in bandgap value of around 0.56 eV in the heterostructure led to an improvement in resistance of 100 times compared to the 'off' state. The hysteretic *I*-*V* characteristics, however, remained relatively consistent after three cycles, demonstrating stable and reversible nonvolatile resistance switching. The critical voltage of polarization switching of approximately 4.5 V is considerably higher than that from the PFM measurement (less than 2 V). This is because the effective imposed area (several square microns) of applied voltage in the heterostructure is larger than the contact area of the tip (hundreds of nanometers) on the sample in the PFM test. Thus, a much higher reversal voltage is required to obtain the same electric field for polarization. High-performance memory properties with an on/off ratio exceeding 100 and relatively small switching voltage of the vertical α-In_2Se_3/WSe_2 heterostructure device may provide a new approach by which 2D ferroelectric semiconductors can be applied to the development of multifunctional nanodevices [28].

4 Conclusion

We have synthesized high-quality single-crystal α-In_2Se_3, the characteristics of which have been confirmed by Raman spectroscopy and HRTEM. PFM measurements demonstrated that layered nanoflakes of α-In_2Se_3 were stable at room-temperature and exhibited out-of-plane ferroelectricity. The scanned ferroelectric domains displayed opposite polarization orientations and the tested amplitude and phase curves exhibited hysteresis during the reversal process. After assembling α-In_2Se_3/WSe_2 vertical heterostructures, we noted switchable diode effects and nonvolatile memory phenomena. I-V behavior could be reversed by applying opposite voltages between the heterostructure and the sweeping I-V curves show hysteresis and resistance switches. This α-In_2Se_3/WSe_2 heterostructure memory device with stable and reversible nonvolatile resistance switching is characterized by superior performance with an on/off ratio exceeding 100 and a relatively small switching voltage. Nonvolatile memory based on vdW ferroelectric heterostructure should provide new opportunities and a novel platform for utilizing and developing 2D ferroelectric materials for information storage.

Acknowledgements This work was supported by National Natural Science Foundation of China (Grant Nos. 61622406, 61571415), National Key Research and Development Program of China (Grant Nos. 2017YFA0207500, 2016YFB0700700), and Strategic Priority Research Program of Chinese Academy of Sciences (Grant No. XDB30000000).

References

1 Garcia V, Fusil S, Bouzehouane K, et al. Giant tunnel electroresistance for non-destructive readout of ferroelectric states. Nature, 2009, 460: 81–84
2 Wen Z, Li C, Wu D, et al. Ferroelectric-field-effect-enhanced electroresistance in metal/ferroelectric/semiconductor tunnel junctions. Nat Mater, 2013, 12: 617–621
3 Xu R J, Liu S, Grinberg I, et al. Ferroelectric polarization reversal via successive ferroelastic transitions. Nat Mater, 2015, 14: 79–86
4 Ge R J, Wu X H, Kim M, et al. Atomristor: nonvolatile resistance switching in atomic sheets of transition metal dichalcogenides. Nano Lett, 2018, 18: 434–441
5 Scott J F. Applications of modern ferroelectrics. Science, 2007, 315: 954–959
6 Morris M R, Pendlebury S R, Hong J, et al. Effect of internal electric fields on charge carrier dynamics in a ferroelectric material for solar energy conversion. Adv Mater, 2016, 28: 7123–7128
7 Jones A M, Yu H, Ghimire N J, et al. Optical generation of excitonic valley coherence in monolayer WSe_2. Nat Nanotech, 2013, 8: 634–638
8 Castro Neto A H, Guinea F, Peres N M R, et al. The electronic properties of graphene. Rev Mod Phys, 2009, 81: 109–162
9 Wang Y X, Xu N, Li D Y, et al. Thermal properties of two dimensional layered materials. Adv Funct Mater, 2017, 27: 1604134
10 Huang B, Clark G, Navarro-Moratalla E, et al. Layer-dependent ferromagnetism in a van der Waals crystal down to the monolayer limit. Nature, 2017, 546: 270–273
11 Si M, Su C J, Jiang C, et al. Steep-slope hysteresis-free negative capacitance MoS_2 transistors. Nat Nanotech, 2018, 13: 24–28
12 Wang X D, Zhou J, Song J H, et al. Piezoelectric field effect transistor and nanoforce sensor based on a single ZnO nanowire. Nano Lett, 2006, 6: 2768–2772
13 Tian B B, Liu L, Yan M, et al. A robust artificial synapse based on organic ferroelectric polymer. Adv Electron Mater, 2019, 5: 1800600
14 Boyn S, Grollier J, Lecerf G, et al. Learning through ferroelectric domain dynamics in solid-state synapses. Nat Commun, 2017, 8: 14736

15 Chang K, Liu J W, Lin H C, et al. Discovery of robust in-plane ferroelectricity in atomic-thick SnTe. Science, 2016, 353: 274–278

16 Si M W, Liao P Y, Qiu G, et al. Ferroelectric field-effect transistors based on MoS_2 and $CuInP_2S_6$ two-dimensional van der Waals heterostructure. ACS Nano, 2018, 12: 6700–6705

17 Liu F C, You L, Seyler K L, et al. Room-temperature ferroelectricity in $CuInP_2S_6$ ultrathin flakes. Nat Commun, 2016, 7: 12357

18 Ding W J, Zhu J B, Wang Z, et al. Prediction of intrinsic two-dimensional ferroelectrics in In_2Se_3 and other III_2-VI_3 van der Waals materials. Nat Commun, 2017, 8: 14956

19 Zhou J D, Zeng Q S, Lv D H, et al. Controlled synthesis of high-quality monolayered α-In_2Se_3 via physical vapor deposition. Nano Lett, 2015, 15: 6400–6405

20 Tao X, Gu Y. Crystalline-crystalline phase transformation in two-dimensional In_2Se_3 thin layers. Nano Lett, 2013, 13: 3501–3505

21 Cui J L, Wang L, Du Z L, et al. High thermoelectric performance of a defect in α-In_2Se_3-based solid solution upon substitution of Zn for In. J Mater Chem C, 2015, 3: 9069–9075

22 Ho C H, Lin M H, Pan C C. Optical-memory switching and oxygen detection based on the CVT grown γ- and α-phase In_2Se_3. Sens Actuat B-Chem, 2015, 209: 811–819

23 Cui C, Hu W J, Yan X, et al. Intercorrelated in-plane and out-of-plane ferroelectricity in ultrathin two-dimensional layered semiconductor In_2Se_3. Nano Lett, 2018, 18: 1253–1258

24 Xiao J, Zhu H Y, Wang Y, et al. Intrinsic two-dimensional ferroelectricity with Dipole locking. Phys Rev Lett, 2018, 120: 227601

25 Zhou Y, Wu D, Zhu Y H, et al. Out-of-plane piezoelectricity and ferroelectricity in layered α-In_2Se_3 nanoflakes. Nano Lett, 2017, 17: 5508–5513

26 Wan S Y, Li Y, Li W, et al. Room-temperature ferroelectricity and a switchable diode effect in two-dimensional α-In_2Se_3 thin layers. Nanoscale, 2018, 10: 14885–14892

27 Lewandowska R, Bacewicz R, Filipowicz J, et al. Raman scattering in α-In_2Se_3 crystals. Mater Res Bull, 2001, 36: 2577–2583

28 Tian B B, Wang J L, Fusil S, et al. Tunnel electroresistance through organic ferroelectrics. Nat Commun, 2016, 7: 11502